Optimization of Magneto-Hydrodynamic Control of Diffuser Flows Using Micro-Genetic Algorithms and Least-Squares Finite Elements

Brian H. Dennis [1]

Department of Aerospace Engineering, 233 Hammond, The Pennsylvania State University, University Park, PA 16802, U.S.A
E-mail address: bhd102@psu.edu

George S. Dulikravich [2]

Department of Mechanical and Aerospace Engineering, Box 19018, The University of Texas at Arlington, Arlington, TX 76019, U.S.A
E-mail address: gsd@uta.edu

Abstract

In this paper we consider the problem of multidisciplinary design and optimization (MDO) of a diffuser for a steady, incompressible magnetohydrodynamic (MHD) flow. Given a fixed diffuser shape, the optimizer should find the distribution of the wall magnets that will maximize the static pressure increase from inlet to outlet. This design problem is solved through the use of a genetic algorithm based optimization program coupled with a finite element based MHD simulation program. For MHD simulation, a least-squares finite element method (LSFEM) based program has been developed. The use of LSFEM allows the use of equal order approximation functions for all unknowns and is stable for high Reynolds numbers. Optimization was accomplished using a micro-genetic algorithm (GA) based program. The micro-GA is capable of searching the design space with a population much smaller than that required by classical GA. The optimization was performed on a parallel computer composed of commodity PC components. Results show that an applied magnetic field with the proper strength and distribution can significantly improve the static pressure rise over the case of no magnetic field.

Key Words: Magnetohydrodynamics, least-squares finite element method, genetic algorithms, optimization, distributed parallel computing

[1] Graduate research assistant.
[2] Professor.

1 Introduction

In this paper we consider the problem of multidisciplinary design and optimization (MDO) of a diffuser for a steady, incompressible magnetohydrodynamic (MHD) flow. The problem can be stated as follows: given a fixed geometry, the optimizer should find the distribution of the wall magnets that will produce the most efficient diffuser design. In this case, efficiency is measured by total increase in static pressure, which should be maximized. This design problem is solved through the use of a genetic algorithm based optimization program coupled with a finite element based MHD simulation program.

The least-squares finite element method (LSFEM) has been applied successfully to steady and unsteady incompressible 2D flows [6,13]. There are several advantages to using LSFEM some of which will be mentioned here. First, the LSFEM produces symmetric positive definite systems of algebraic equations that can be solved efficiently by simple iterative methods such as the preconditioned conjugate gradient method. Furthermore, the LSFEM can be applied to equations or systems of equations of any type without any special treatment which makes it an ideal method for use in multidisciplinary problems involving various kinds of physics, such as MHD. Another benefit of using LSFEM is that it is not subject to the restrictive *inf-sup* condition [6]. Equal order approximation functions can be employed for all unknowns without causing instability.

The optimization method is based on a micro-genetic algorithm (GA). This methods allows the optimizer to search the design space with a much smaller population than that required by the classical GA.

The GA typically requires many function evaluations to find an optimum solution. In this case, computational cost is minimized through the use of a distributed memory parallel computer based on commodity hardware components. The combination of analysis and optimization software based on LSFEM and micro-GA and cheap commodity component based parallel computers make the solution of MDO problems tractable.

2 Simulation of MHD Flows

A magnetohydrodynamic flow can be basically described as the flow of an electrically conducting incompressible fluid through an applied magnetic field. The following sections give an overview of the equations governing MHD flows as well as the LSFEM numerical method that is used for numerical simulation of such flows.

2.1 Governing Equations

The steady viscous incompressible MHD flow can be described by the Navier-Stokes equations combined with the Maxwell's equations.

$$\begin{aligned} \nabla \cdot \mathbf{V} &= 0 && (1)\\ \rho \mathbf{V} \cdot \nabla \mathbf{V} - \eta \nabla^2 \mathbf{V} + \nabla P - \sigma \mathbf{V} \times \mathbf{B} \times \mathbf{B} &= 0 && (2)\\ \nabla \cdot \mathbf{B} &= 0 && (3)\\ \nabla \times \mathbf{B} &= \mu\sigma \mathbf{V} \times \mathbf{B} && (4) \end{aligned}$$

Here, $\mathbf{V}$ is the fluid velocity, ρ is the fluid density, P is the hydrodynamic pressure, η is the coefficient of viscosity, $\mathbf{B}$ is the magnetic flux density, μ is the magnetic permeability coefficient, and σ is the electrical conductivity of the fluid. Only the presence of a steady magnetic field is considered here so the equations and terms in Maxwell's equations relating to the electric field are omitted. Simulations of fluid flow with applied magnetic and electric fields would require a much more complicated mathematical model [7].

For computations, we use the corresponding nondimensional form of the above equations

$$\begin{aligned} \nabla^* \cdot \mathbf{V}^* &= 0 && (5)\\ \mathbf{V}^* \cdot \nabla^* \mathbf{V}^* - \frac{1}{Re} \nabla^{*2} \mathbf{V}^* + \nabla^* P^* - \frac{Ht^2}{Re} \mathbf{V}^* \times \mathbf{B}^* \times \mathbf{B}^* &= 0 && (6)\\ \nabla^* \cdot \mathbf{B}^* &= 0 && (7)\\ \nabla^* \times \mathbf{B}^* &= Rm \mathbf{V}^* \times \mathbf{B}^* && (8) \end{aligned}$$

where $V^* = V\,U_0^{-1}$, $B^* = B\,B_0^{-1}$, $P^* = P\,\rho^{-1}U_0^{-2}$, $x^* = x\,L_0^{-1}$, $y^* = y\,L_0^{-1}$. Here, L_0 is the reference length, U_0 is the reference speed, and B_0 is the reference magnetic flux density. For convenience the $*$ superscript will be dropped for the remainder of the paper.

The nondimensional numbers are given by:

$$\begin{aligned} \text{Reynolds number} \qquad & Re = \frac{\rho U_0 L_0}{\eta}\\ \text{Magnetic Reynolds number} \qquad & Rm = \mu\sigma U_0 L_0\\ \text{Hartmann number} \qquad & Ht = L_0 B_0 \sqrt{\frac{\sigma}{\eta}} \end{aligned}$$

2.2 Least-Squares Finite Element Method

The system of partial differential equations described in section 2.1 is discretized using the least squares finite element method. We first look at the LSFEM for a general linear first-order system.

$$[L]\mathbf{u} = \mathbf{f} \tag{9}$$

where

$$[L] = [A_1]\frac{\partial}{\partial x} + [A_2]\frac{\partial}{\partial y} + [A_3] \tag{10}$$

The residual of the system is represented by $\mathbf{R}$.

$$\mathbf{R}(\mathbf{u}) = [L]\mathbf{u} - \mathbf{f} \tag{11}$$

We now define the following least squares functional I over the domain Ω

$$I(\mathbf{u}) = \int_{\Omega} \mathbf{R}(\mathbf{u})^T \cdot \mathbf{R}(\mathbf{u})\, dx\, dy \tag{12}$$

The weak statement is then obtained by taking the variation of I with respect to $\mathbf{u}$ and setting the result equal to zero.

$$\delta I(\mathbf{u}) = \int_{\Omega} ([L]\delta\mathbf{u})([L]\mathbf{u} - \mathbf{f})\, dx\, dy = 0 \tag{13}$$

Using equal order shape functions, ϕ_i, for all unknowns, the vector $\mathbf{u}$ is written as

$$\mathbf{u} = \sum_{i=1}^{n} \phi_i \{u_1, u_2, u_3, ..., u_m\}_i^T \tag{14}$$

where $\{u_1, u_2, u_3, ..., u_m\}_i$ are the nodal values at the ith node of the finite element. Introducing the above approximation for $\mathbf{u}$ into the weak statement leads to a linear system of algebraic equations

$$[K]\mathbf{U} = \mathbf{F} \tag{15}$$

where $[K]$ is the stiffness matrix, $\mathbf{U}$ is the vector of unknowns, and $\mathbf{F}$ is the force vector.

2.3 LSFEM for Magnetohydrodynamics

Use of LSFEM for systems of equations that contain higher order derivatives is usually difficult due to the higher continuity restrictions imposed on the approximation functions. For this reason, it is usually more convenient to transform the system into an equivalent first order form before applying LSFEM. For the case of magnetohydrodynamics, the second order derivatives are transformed by introducing vorticity, ω, as an additional unknown.

$$\nabla \cdot \mathbf{V} = 0 \tag{16}$$

$$\mathbf{V} \cdot \nabla \mathbf{V} + \frac{1}{Re} \nabla \times \omega + \nabla P - \frac{Ht^2}{Re} \mathbf{V} \times \mathbf{B} \times \mathbf{B} = 0 \tag{17}$$

$$\omega - \nabla \times \mathbf{V} = 0 \tag{18}$$

$$\nabla \cdot \mathbf{B} = 0 \tag{19}$$

$$\nabla \times \mathbf{B} = Rm \mathbf{V} \times \mathbf{B} \tag{20}$$

We consider a two-dimensional problem only and write the above system in the general form of a first- order system (9). Although the LSFEM is perfectly capable of treating the entire system written in (16)-(20), it was found to be more economical to solve the fluid and magnetic field equations separately, in an iterative manner. Here, a general form first-order system is written for the fluid system (16)-(18) and denoted by the superscript $fluid$. A first-order system is also written in general form for the magnetic field equations (19)-(20) and is denoted by the superscript mag. In addition, the nonlinear convective terms in the fluid equations are linearized with Newton's method leading to a system suitable for treatment with the LSFEM described in section 2.2.

$$\left[A_1^{fluid}\right] = \begin{bmatrix} 1 & 0 & 0 & 0 \\ u_0 & 0 & 1 & 0 \\ 0 & u_0 & 0 & -\frac{1}{Re} \\ 0 & -1 & 0 & 0 \end{bmatrix}, \qquad \left[A_2^{fluid}\right] = \begin{bmatrix} 0 & 1 & 0 & 0 \\ v_0 & 0 & 0 & \frac{1}{Re} \\ 0 & v_0 & 1 & 0 \\ 1 & 0 & 0 & 0 \end{bmatrix},$$

$$\left[A_3^{fluid}\right] = \begin{bmatrix} 0 & 0 & 0\,0 \\ \frac{Ht^2}{Re} B_{y0}^2 + \frac{\partial u_0}{\partial x} & -\frac{Ht^2}{Re} B_{x0} B_{y0} + \frac{\partial u_0}{\partial y} & 0\,0 \\ -\frac{Ht^2}{Re} B_{x0} B_{y0} + \frac{\partial v_0}{\partial x} & \frac{Ht^2}{Re} B_{x0}^2 + \frac{\partial v_0}{\partial y} & 0\,0 \\ 0 & 0 & 0\,1 \end{bmatrix},$$

$$\mathbf{f}^{fluid} = \begin{Bmatrix} 0 \\ u_0 \frac{\partial u_o}{\partial x} + v_0 \frac{\partial u_o}{\partial y} \\ u_0 \frac{\partial v_o}{\partial x} + v_0 \frac{\partial v_o}{\partial y} \\ 0 \end{Bmatrix}, \qquad \mathbf{u}^{fluid} = \begin{Bmatrix} u \\ v \\ p \\ \omega \end{Bmatrix} \tag{21}$$

$$[A_1^{mag}] = \begin{bmatrix} 1 & 0 \\ 0 & 1 \end{bmatrix}, [A_2^{mag}] = \begin{bmatrix} 0 & 1 \\ -1 & 0 \end{bmatrix}, [A_3^{mag}] = \begin{bmatrix} 0 & 0 \\ Rm\, v_0 & -Rm\, u_0 \end{bmatrix},$$

$$\mathbf{f}^{mag} = \begin{Bmatrix} 0 \\ 0 \end{Bmatrix}, \qquad \mathbf{u}^{mag} = \begin{Bmatrix} B_x \\ B_y \end{Bmatrix} \tag{22}$$

A solution satisfying both of the above systems of equations can be found by using a simple iterative process. First, the system in (21) is solved with the magnetic field given from an initial guess or from the previous iteration. Here quantities taken from the previous iteration are designated with the subscript 0. Next,the system given in (22) is solved using the recently calculated velocity field. This process is repeated until a specified convergence tolerance is reached. For most cases considered in this paper, reduction of the residual norm of both systems by 3.5 orders of magnitude was achieved in less than 5 iterations.

2.4 Verification of Accuracy

The accuracy of the LSFEM for MHD was tested against known analytic solutions for Poisuille-Hartmann flow. The Poisuille-Hartmann flow is a 1-D flow of a conducting and viscous fluid between two stationary plates with a uniform external magnetic field applied orthogonal to the plates. Assuming the walls are at $y = \pm L$ and that fluid velocity on the walls is zero and that the fluid moves in the x-direction under the influence of a constant pressure gradient, then the velocity profile is given by [12,11]

$$u(y) = \frac{\rho H t}{\sigma B_y^2} \frac{\partial p}{\partial x} \left(\frac{\cosh(Ht) - \cosh(\frac{Hty}{L})}{\sinh(Ht)} \right) \tag{23}$$

The movement of the fluid induces a magnetic field in the x-direction and is given by

$$B_x(y) = \frac{B_y Rm}{Ht} \left(\frac{\sinh(\frac{Hty}{L}) - (\frac{y}{L}\sinh(Ht)}{\cosh(Ht) - 1} \right) \tag{24}$$

A test case was run using the parameters given in Table 1 and with a mesh composed of 2718 parabolic triangular elements. Figure 1 shows the computed and analytical results for the velocity profile. Figure 2 shows the computed and analytical results for the induced magnetic field. For both cases, one can see that the agreement between the analytical solution and the LSFEM solution is excellent.

3 Genetic Algorithm

Genetic algorithms are heuristic global optimization methods that are based on the process of natural selection. Starting from a randomly generated population of designs, the optimizer seeks to produce improved designs from one generation to the next. This is accomplished by exchanging genetic information between designs in the current population in what is referred to as the crossover operation. Hopefully this crossover produces improved designs which are then used to populate the next generation.

3.1 Micro-GA

The well know problem of premature convergence for classical GA's can be avoided through the use of the micro-genetic algorithm method [8]. The micro GA starts with a very small random population. The GA is used in the normal fashion on this small population until the binary strings of each individual differs from that of the best individual by less than some specified percentage. In this paper, a value of 5 percent was used for all cases. At this point the entire population, except for the best individual, is replaced by random designs. For population of 15 individuals with 9-bit strings, these restarts usually happen after 15-20 generations. This periodic infusion of new genetic material allows the micro GA to search the function space using a very small population. It will also keep the population from being dominated by designs corresponding to a local minimum found early in the optimization process.

3.2 Parallel GA

Genetic algorithms are robust search techniques that are capable of avoiding local minimum. However, for a complex function space with many local minima it may take many generations before the global minimum is located. This translates into hundreds and possibly thousands of function evaluations. If the function evaluation is expensive, such as a finite element analysis, it

many take days or weeks to complete an optimization with a GA on a single workstation. However, one of the main advantages in using GA's is the fact that they are inherently parallel algorithms. Little effort is needed to modify an existing GA to make use of a parallel computer. The simplest way to parallelize a GA, and the method used in this paper, is to use the synchronous master-slave model [5]. Basically, the master processor does all computations relating to the actual GA, such as selection and crossover operations. The slave processors are tasked by the master to complete a function analysis of a given design and return the computed fitness. This model works well if all function analyses require the same amount of computation effort and have a long processing time relative to the amount of communication time needed to exchange information between master and slave. In addition, it has recently become very affordable to create powerful parallel computers from commodity personal computer components [10]. Such machines should eventually make the use of GA's with finite element analysis common place in engineering design.

3.3 Verification of Accuracy

An optimization of a 2D analytic function was used to verify the accuracy of the micro-GA. This test function is given as:

$$\begin{aligned} a = x - 1.0 \quad b = y - 2.0 \quad d = aa + bb + .5ab \\ e = \exp(-d/8.0) \quad g = \cos(4.0\sqrt{d}) \\ f = 1.0 - eg \end{aligned} \tag{25}$$

Figure 3 shows a graphical depiction of the function to be minimized. This test problem is difficult for a traditional gradient based optimizer since it has many false minima and would require an initial guess very close to the global minimum. A micro GA based code [3,2] was used with a population of 5, uniform crossover, a 50% probability of crossover, tournament selection, and no mutation. Both design variables were encoded with 9-bit strings and were limited to the range -5 to 5. The global minima for this function is located at $(1.0, 2.0)$. After 500 generations, the best design found by the GA was located at $(1.0, 2.0196)$.

4 Numerical Results

A parallel micro GA based code [3,2,4] was used to find the magnetic field strength and distribution along the walls of a given diffuser that would maxi-

mize the static pressure increase from inlet to exit.

The diffuser shape is shown in figure 4. The inlet height is 0.5 m and the outlet height is 3.0 m and length is 1.5 m. The physical parameters used are given in table 2. The Reynolds number is 486, based on the outlet height.

The magnetic field distribution along the diffuser bottom wall was parameterized with two B-splines, one spline for the normal component and one spline for the tangential component. It should be noted that only the distribution along the bottom wall was parameterized since the top wall distribution was assumed to be mirror image of the bottom, but with antisymmetric direction. Seven control points were used for each spline. The control points were encoded with 9-bit binary strings and were allowed to move vertically from -1.0 to 1.0 and horizontally along the full length of the diffuser except the end control points which were fixed. A 10-bit string was used to encode the magnetic field strength,B_0, which was allowed to vary from 0 to 1.2 Telsa. Altogether, a total of 20 design variables were used.

The MHD analysis was performed by a LSFEM code written in C/C++. A hybrid triangle and quadrilateral mesh of parabolic elements was used [9]. A typical mesh is shown in figure 5. A parabolic velocity profile was specified at the upstream boundary while a uniform static pressure was specified at the downstream boundary, which was located several diffuser exit heights away from the diffuser outlet. A no-slip boundary condition for velocity was specified at the walls. Zero normal component of the magnetic field was enforced on all walls except those belonging to the diffuser; there the magnetic field components were specified. The fitness of a design, which is static pressure rise in this case, was determined by integrating the static pressure at the diffuser outlet ($x = 1.5\ m$) and subtracting it from the integrated static pressure at the diffuser inlet ($x = 0\ m$). The sparse linear system for both the magnetic field and fluid flow were solved with a sparse LU code [1] at each nonlinear iteration. Convergence history for a typical analysis is shown in figure 6.

All computations were made on a distributed parallel computer composed of 32 Pentium II 400 MHz processors. All communications were done using the MPICH library. Two optimizations runs were made simultaneously, each starting from different random populations and each using 16 processors. Each used micro GA, a population size of 15, uniform crossover, a 50% probability of crossover, tournament selection, and no mutation. In about 30 hours, both optimization runs completed 100 generations.

Figures 7–8 show the average fitness and the fitness of the best population member as a function of generation for both micro-GA optimization runs. The locations of population restarts are clearly visible in the plots of average fitness. Both runs seem to be converging to the same design, though run 2 found a

slightly better answer. By generation 100, run 1 achieved a pressure increase of .207 Pa and run 2 achieved a pressure increase of .228 Pa. For comparison, the diffuser without an applied magnetic field achieved a pressure increase of .05 Pa. Figure 11 shows the streamlines for the diffuser with the optimized applied magnetic field. For comparison, figure 10 shows the streamlines for the diffuser with no applied magnetic field.

We would also like to point out that it is not difficult to design by hand a magnetic field that will completely suppress the vortices. Streamlines for such a configuration is shown in figure 12. One would think that this would result in a large pressure increase but, in fact, the pressure drops dramatically as shown in figure 13. The distributed magnetic field that will suppress the vortices is so strong (approximately 2.0 Tesla in this case) that it exerts a braking effect on the fluid similar to what occurs in Poisuille-Hartmann flow. The pressure drop due to the magnetic braking far outweighs the pressure increase due to the suppression of the vortices. This demonstrates why optimization is critical for finding improvements in design situations that include complex interactions among multiple physics.

5 Conclusion

A MHD simulation code has been developed based on the LSFEM. It shows excellent agreement with known analytic solutions for Poisuille-Hartmann flow. The MHD simulation was coupled to a micro-GA code for the optimization of magnetic field strength and distribution on the walls of a given diffuser. Two simultaneous optimization runs were made successfully on a commodity component based parallel computer. The GA optimizer was able to design a magnetic field that when applied to the wall of the diffuser increased the static pressure rise. The pressure was increased by more than a factor of four compared to a diffuser with no applied magnetic field. These results show that GA's coupled together with LSFEM and parallel computers are capable of performing optimization involving different disciplines in a timely manner.

References

[1] Satish Balay, William D. Gropp, Lois Curfman McInnes, and Barry F. Smith. PETSc 2.0 users manual. Technical Report ANL-95/11 - Revision 2.0.24, Argonne National Laboratory, 1999.

[2] David L. Carroll. Chemical laser modeling with genetic algorithms. *AIAA Journal*, 34(2):338–346, February 1996.

[3] David L. Carroll. Genetic algorithms and optimizing chemical oxygen-iodine lasers. In H. Wilson, R. Batra, C. Bert, A. Davis, R. Schapery, D. Stewart, and F. Swinson, editors, *Developments in Theoretical and Applied Mechanics*, volume XVIII, pages 411–424. School of Engineering, The University of Alabama, 1996.

[4] G. S. Dulikravich, T. J. Martin, B. H. Dennis, and N. F. Foster. *EUROGEN'99 - Evolutionary Algorithms in Engineering and Computer Science: Recent Advances and Industrial Applications*, chapter 12, pages 233–259. John Wiley and Sons, 1999.

[5] David E. Goldberg. *Genetic Algorithms in Search, Optimization, and Machine Learning*. Addison-Wesley Publishing Company, Inc., Reading, MA, 1989.

[6] Bo-Nan Jiang. A least-squares finite element method for incompressible navier-stokes problems. *International Journal for Numerical Methods in Fluids*, 14:843–859, 1992.

[7] H.-J. Ko and G. S. Dulikravich. A fully non-linear theory of electro-magneto-hydrodynamics. In D.A. Siginer and D.D. Kee, editors, *Symposium on Rheology and Fluid Mechanics of Nonlinear Materials*. ASME, Anaheim, CA, Nov. 1998 ASME FED-Vol. 246, MD-Vol. 81, pp. 173–182, 1998. Also to appear in Int. J. of Non-linear Mechanics, 2000.

[8] K. Krishnakumar. Micro-genetic algorithms for stationary and non-stationary function optimization functiob. In *SPIE: Intelligent Control and Adaptive Systems*, volume 1196, Philadelphia, PA, 1989.

[9] D. L. Marcum and N. P. Weatherhill. Unstructured grid generation using iterative point insertion and local reconnection. *AIAA Journal*, 33(9):1619–1625, September 1995.

[10] Daniel Ridge, Donald Becker, Phillip Merkey, and Thomas Sterling. Beowulf: Harnessing the power of parallelism in a pile-of-pcs. In *IEEE Aerospace Applications Conference Proceedings*, volume 2, pages 79–91, New York, Feb 1-2 1997. IEEE.

[11] Nizar Ben Salah, Azzeddine Soulaimani, Wagdi G. Habashi, and Michel Fortin. A conservative stabilized finite element method for the magneto-hydrodynamic equations. *International Journal for Numerical Methods in Fluids*, 29:535–554, 1999.

[12] S. S. Sazhin, M. Makhlouf, and T. Ishii. Solutions of magnetohydrodynamic problems based on a conventional computational fluid dynamics code. *International Journal for Numerical Methods in Fluids*, 21:433–442, 1995.

[13] Li Q. Tang and Tate T. H. Tsang. A least-squares finite element method for time-dependant incompressible flows with thermal convection. *International Journal for Numerical Methods in Fluids*, 17:271–289, 1993.

Table 1
Parameters for Poisuille-Hartmann flow test problem

Ht	10
Rm	6×10^{-7}
$L_0\,(m)$	1
$U_0\,(m\,s^{-1})$	0.6
$\eta\,(kg\,m^{-1}s^{-1})$	0.01
$B_0\,(T)$	1
$\mu\,(H\,m^{-1})$	1×10^{-6}
$\partial P/\partial x\,(Pa\,m^{-1})$	0.6
$\sigma\,(\Omega^{-1}m^{-1})$	1

Table 2
Physical parameters for diffuser optimization problem

$\rho\,(kg\ m^{-2})$	1025
$L_0\,(m)$	3
$U_0\,(m\,s^{-1})$	1.58×10^{-4}
$\eta\,(kg\,m^{-1}s^{-1})$	0.001
$\mu\,(H\,m^{-1})$	1×10^{-6}
$\sigma\,(\Omega^{-1}m^{-1})$	4.5

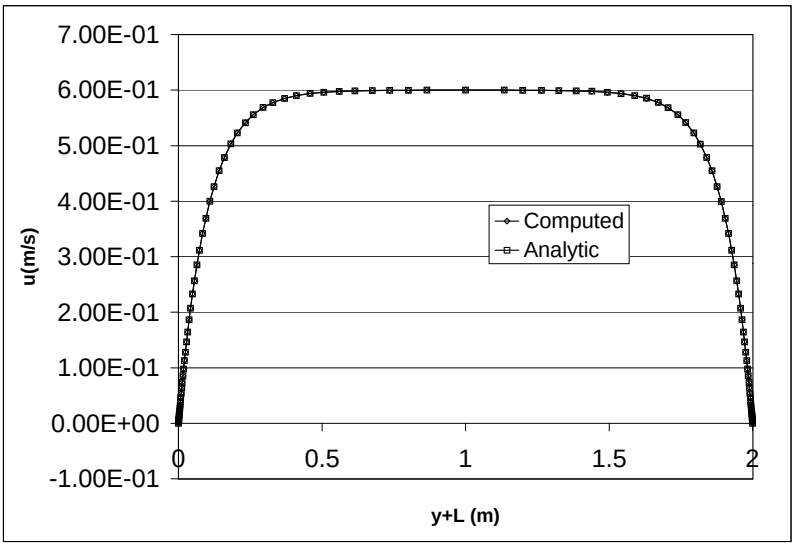

Fig. 1. Computed and analytical values for velocity profile

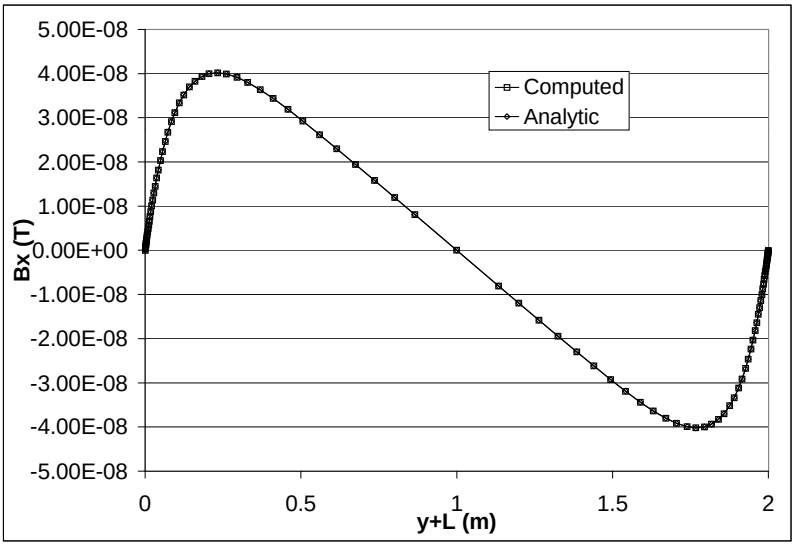

Fig. 2. Computed and analytical values for induced magnetic field

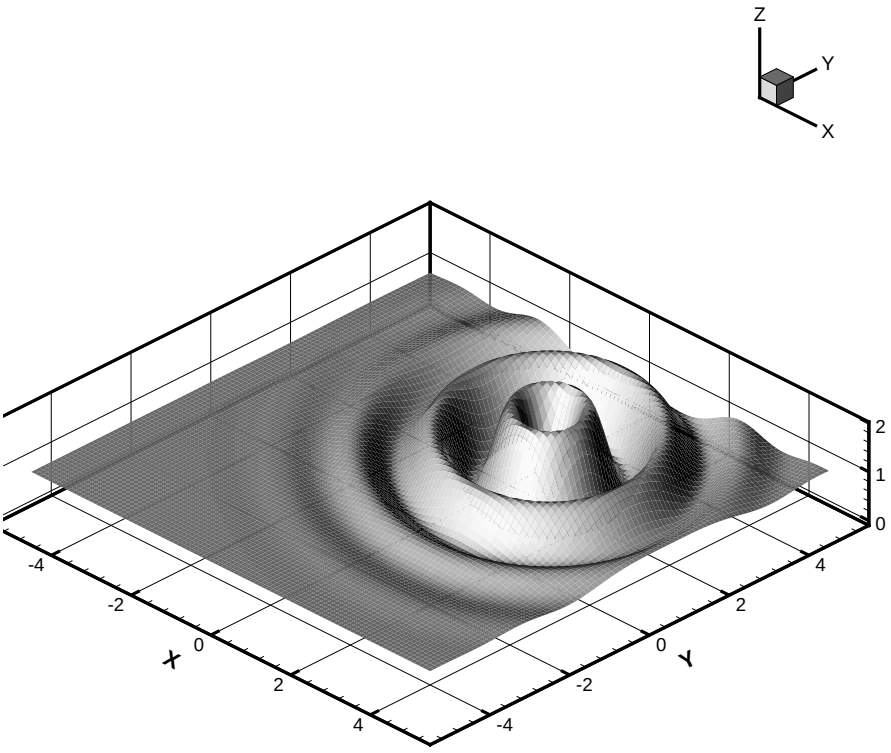

Fig. 3. Test function used to evaluate micro GA

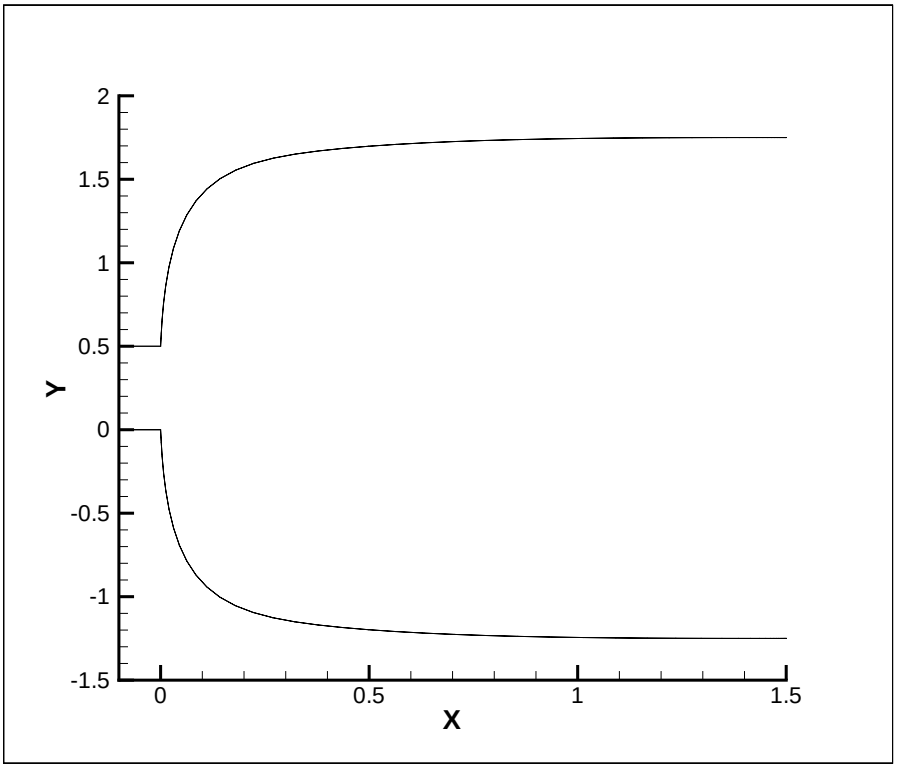

Fig. 4. Given diffuser shape

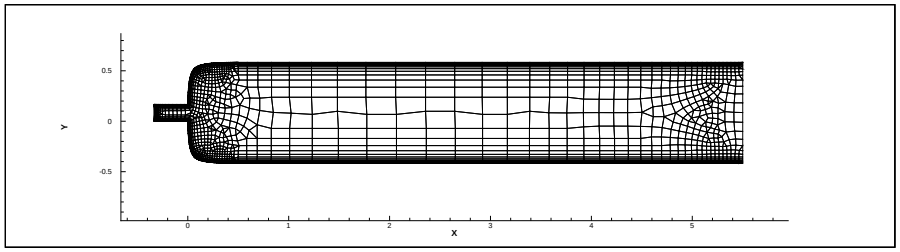

Fig. 5. Mesh for a typical MHD diffuser analysis

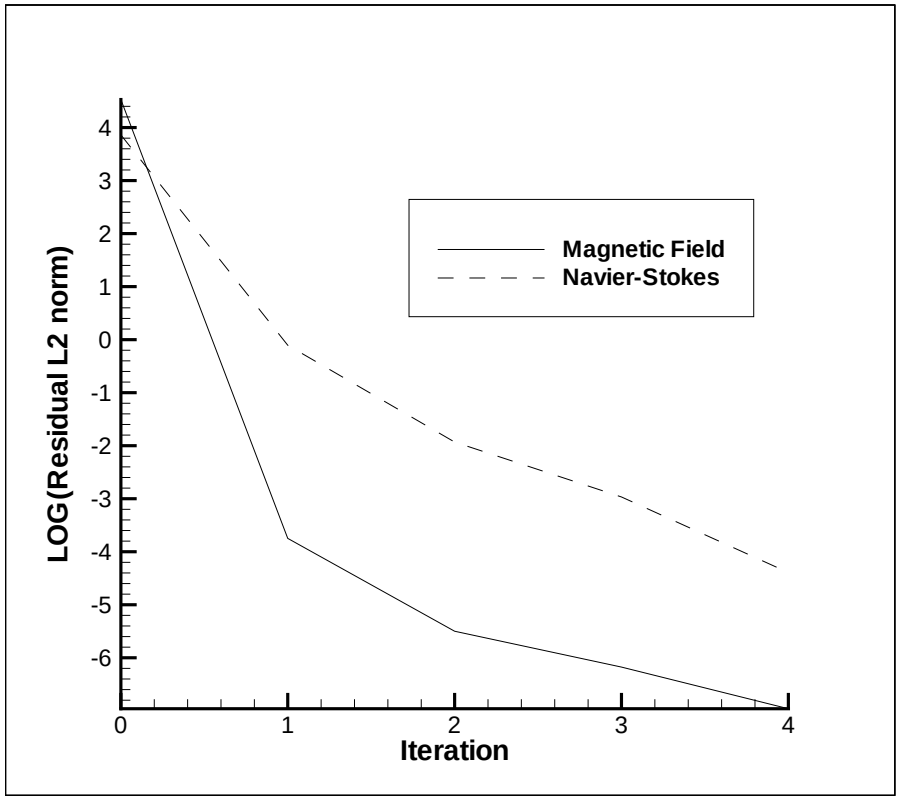

Fig. 6. Convergence history for a typical MHD diffuser analysis

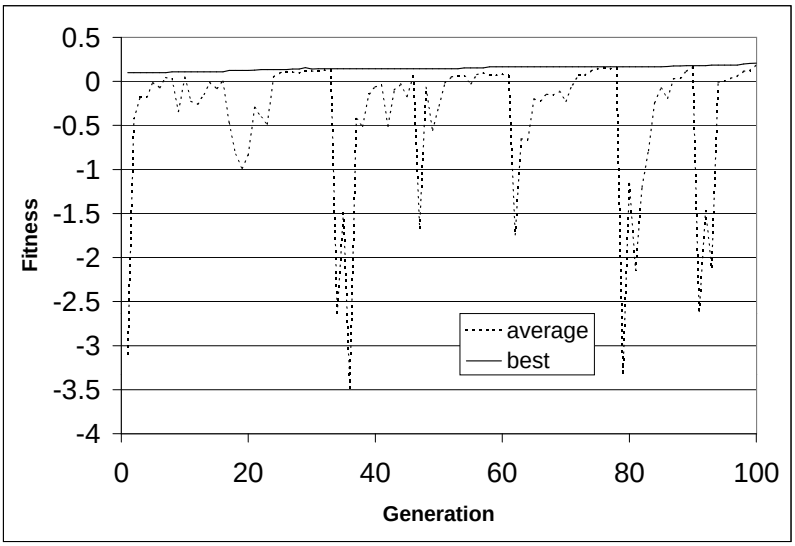

Fig. 7. GA convergence history for run one

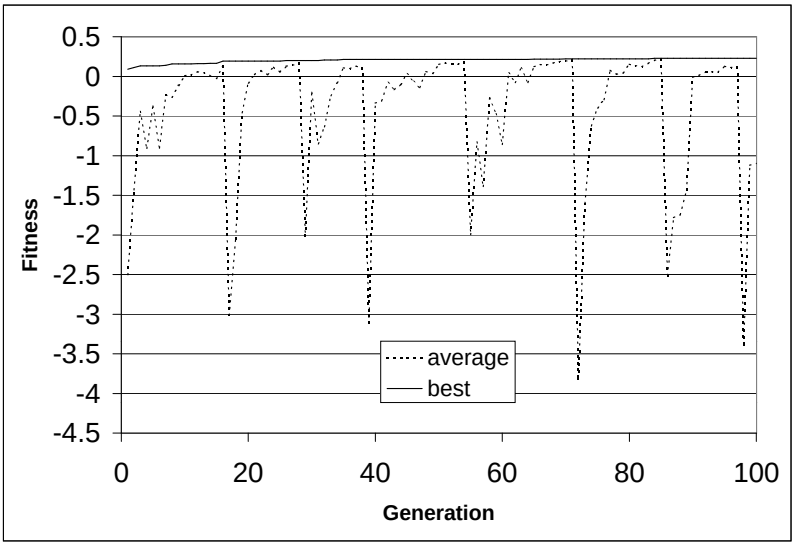

Fig. 8. GA convergence history for run two

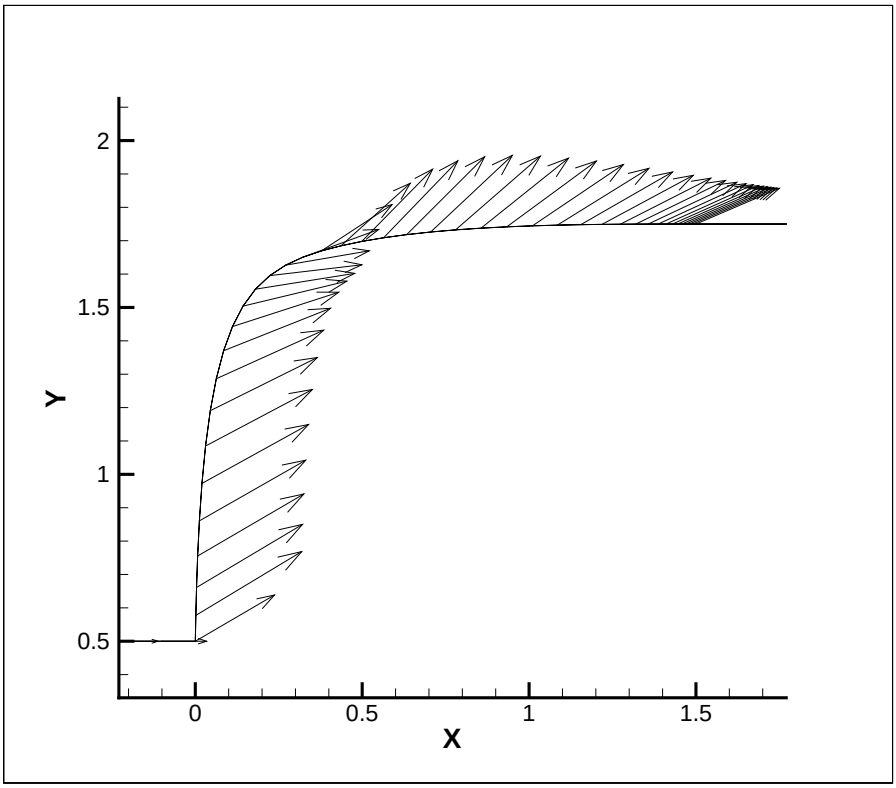

Fig. 9. Optimized magnetic field distribution on top wall

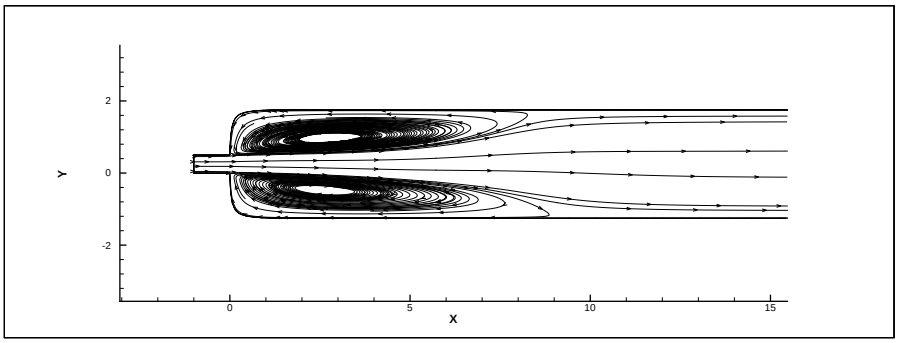

Fig. 10. Streamlines with no applied magnetic field

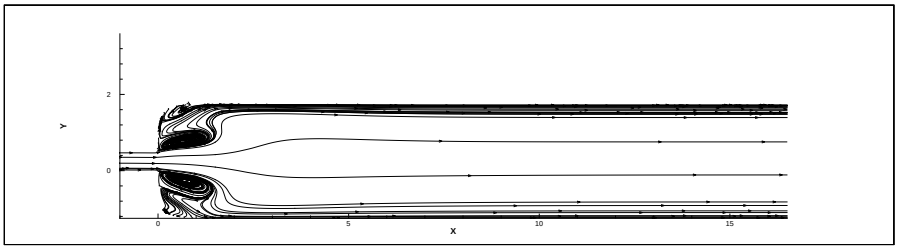

Fig. 11. Streamlines with optimized applied magnetic field

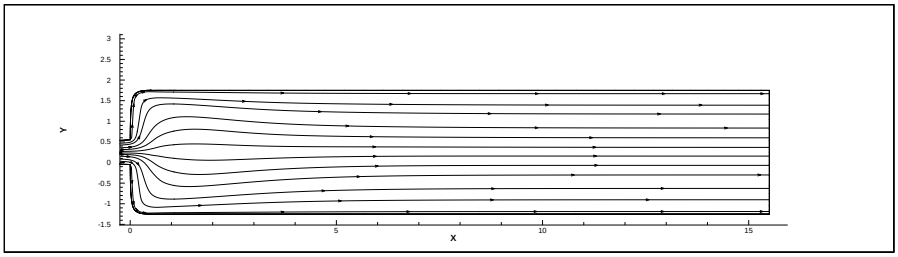

Fig. 12. Streamlines for applied magnetic field that suppresses vortices

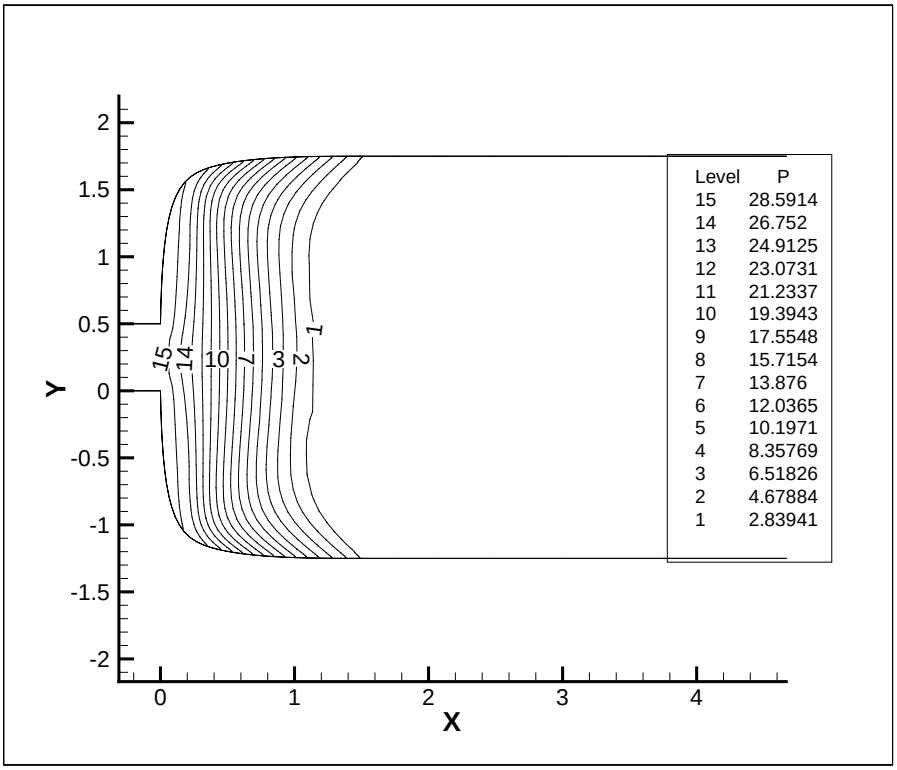

Fig. 13. Static pressure contours for applied magnetic field that suppresses vortices